P4.5 CELLULAR STRUCTURES IN SIMULATED SQUALL LINES WITH MOIST ABSOLUTELY UNSTABLE LAYERS

George H. Bryan and Richard Rotunno
National Center for Atmospheric Research, Boulder, Colorado

1. INTRODUCTION

The structure and intensity of deep convective cells has implications for the development of severe weather in convective lines. For example, deep, intense cells would be more likely to produce large hail. Furthermore, surface wind gusts produced by convective downdrafts would also be more likely to produce severe conditions in cells that are large and intense. In contrast, if convective cells are weaker, one would expect a comparatively lower likelihood of severe weather. Therefore, an understanding of when strong cells are expected, and when they are not, might have value in severe weather prediction.

This paper presents results showing how simple perturbations in the environment can affect the structure and intensity of convective cells in numerical simulations. These results were uncovered during high resolution (grid spacing $\leq$ 125 m) simulations of upshear-tilted mesoscale convective systems (MCSs). These MCSs often have wide (~10 km) and deep (~2 km) layers of air that are saturated and are statically unstable. Often called moist absolutely unstable layers (MAULs), they appear on thermodynamic diagrams as saturated layers that have lapse rates greater than the moist adiabatic lapse rate. They form when the subsaturated, conditionally unstable environmental air is lifted to saturation by the MCS's surface-based cold pool.

We are finding that the existence of a MAUL can affect the structure of cells within the convective region. In a statically unstable layer, perturbations can grow rapidly. Therefore, the perturbations within the environment that flows into MAULs appear to play a role in the structure of cells that develop from the MAUL.

2. SIMULATION DESIGN

The numerical simulations in this study were performed with the model of Bryan and Fritsch (2002). This is a compressible model that uses Runge-Kutta time integration (Wicker and Skamarock 2002) and high-order approximations for advection. In this case, fifth-order advection is used, with no additional artificial diffusion term. The simulations use the Kessler (1969) microphysics scheme and the Deardorff (1980) subgrid turbulence scheme. The grid spacing in all directions is 125 m.

The initial background thermodynamic profile is the analytic sounding of Weisman and Klemp (1982). A line thermal with maximum amplitude of 1.5 K, horizontal radius of 10 km, and vertical radius of 1.5 km is used to initiate a squall line. Random potential temperature (θ) perturbations of $\pm$0.1 K are inserted into this initial thermal in all simulations to allow three-dimensional structure to develop.

For these preliminary simulations, there are no initial winds. Although this environment is not typically associated with severe weather, it was chosen for this preliminary study because it allows for a relatively small domain that is comparatively inexpensive. The results in this environment are symmetric about the initial line thermal used to initiate the squall line. Thus, only one-half of the domain needs to be included in the simulation, where a "mirror" boundary condition is used on one side. Furthermore, the along-line variability in weak-shear simulations is typically very small. Therefore, the along-line width of the domain does not need to be very large to obtain meaningful results. Based on these considerations, the domain was chosen to be 150 km across the squall line (or 300 km, if the "mirrored" half is considered), and is 30 km along the line. The domain depth is 18 km. Based on the interesting findings from this preliminary study, additional simulations with strong environmental shear and larger domains are currently underway.

The results from two simulations are presented in this paper. One is a traditional horizontally homogeneous simulation; no perturbations exist anywhere outside of the initial line thermal. For the second simulation, $\pm$0.1 K θ perturbations are also inserted at *every* grid point in the domain. Thus, the environment that flows into the squall line throughout the simulations has small-amplitude, random thermal perturbations. Because the perturbations have random amplitude, the spectrum of the initial θ field is flat, i.e., it is a white noise spectrum. Thus, perturbations of all spatial scales have equal amplitude.

3. RESULTS

Both simulations run for 3 h, by which time a mature, steady squall line develops. For the simulation without perturbations in the environment (hereafter referred to as NO-PERT), deep clouds continually develop ~20 km behind the surface gust front (Fig. 1a). The individual cumulonimbus clouds are quite strong, with updraft velocities exceeding 35 m s^{-1}, and cloud tops that reach the upper-troposphere. A spatially continuous cloud shield in the 8-10 km layer is being sustained by these deep clouds.

In contrast, the simulation with the random perturbations in the environment (hereafter referred to as

Corresponding author address: George H. Bryan, NCAR/MMM, 3450 Mitchell Lane, Boulder, CO 80301. E-mail: gbryan@ucar.edu

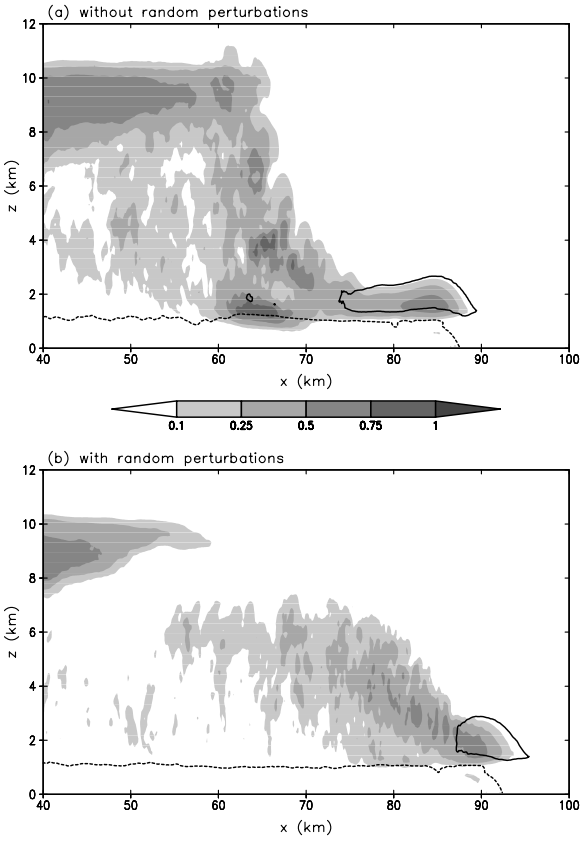

Fig. 1. Line-averaged cross sections at t = 3 h for (a) a simulation without perturbations, and (b) a simulation with small-amplitude random perturbations in the environment. Cloudwater mixing ratio (g kg^{-1}) is shaded. The dashed contour is the –1 K potential temperature perturbation contour. The solid contour encloses the region in which > 50% of the air along the line is moist absolutely unstable.

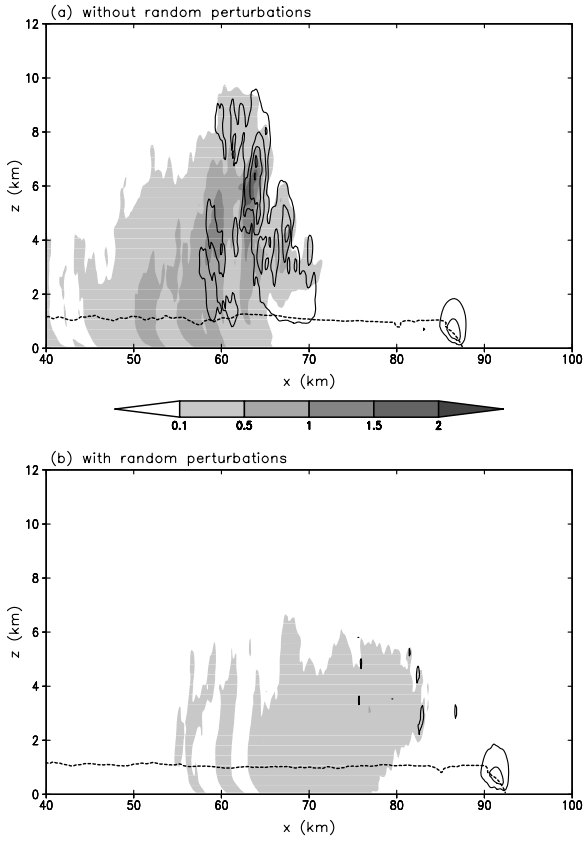

Fig. 2. Line-averaged cross sections at the same time as in Fig. 1, and for the same simulations. Rainwater mixing ratio (g kg^{-1}) is shaded. The dashed contour is the –1 K potential temperature perturbation contour. Vertical velocity is contoured every 1 m s^{-1}, with the zero contour excluded.

WITH-PERT) has a significantly different structure (Fig 1b). The cloud tops ascend more quickly behind the gust front, with cloud top heights > 5 km only 10 km behind the gust front. Furthermore, the maximum cloud tops are only ~7 km above ground (as opposed to > 10 km in NO-PERT). There are some high clouds in the 8-10 km layer for x < 50 km; however, these clouds are left behind by the initial overturning, which was forced by the large initial line thermal.

Patterns of rainwater mixing ratio and vertical velocity are also significantly different (Fig. 2). The rainwater field is deeper in NO-PERT (~10 km) than in WITH-PERT (~6 km). The magnitude of rainwater mixing ratio is also much lower in WITH-PERT. Line-averaged vertical velocity patterns reveal the presence of deep, strong cells in NO-PERT (Fig. 2a), but no indication of a similar pattern in WITH-PERT (Fig. 2b). Interestingly, at this time, the vertical velocity pattern at the cold pool nose is nearly identical in the two simulations (i.e., at x = 88 km in NO-PERT, and x = 92 km in WITH-PERT). Thus, the different character of the cells in the two simulations must be due to something other than cold pool dynamics.

Patterns of vertical velocity (w) at z = 3 km better reveal the different character of the convective cells in the two simulations (Fig. 3). In NO-PERT, the cells are larger and more intense; maximum w values in this simulation are > 35 m s^{-1} in upper-levels. In contrast, the cells in WITH-PERT are smaller and less intense; maximum w values are less than 28 m s^{-1} in the domain. Finally, the average spacing between cells is ~3 km in NO-PERT, but is approximately the minimum resolvable scale (~750 m) in WITH-PERT.

The net effect of these differences is reflected in measures such as total rainfall and precipitation efficiency (Table 1). Total condensation is nearly identical in the two simulations, despite the differences in structure. This result is presumably due to the similar cold pools, which lift essentially the same amount of air to saturation. However, the total rainfall is much lower (by 20%). Consequently, the precipitation efficiency is 20% lower, where precipitation efficiency is defined here as the ratio of water reaching the surface compared to total condensed water. The rainfall rate in WITH-PERT is decreasing in time relative to the rainfall rate in NO-PERT. Thus, the differences in total rainfall and precipitation efficiency are expected to be greater for longer simulations.

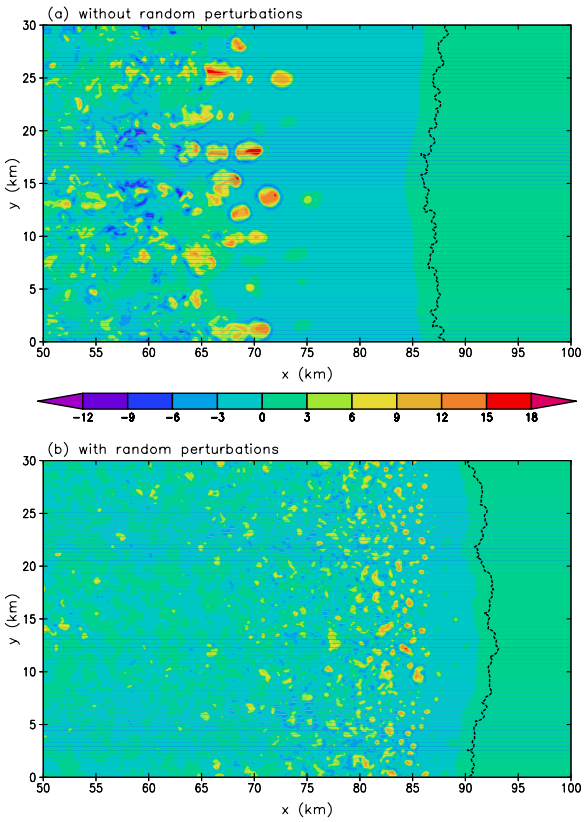

Fig. 3. Vertical velocity at z = 3 km and t = 3 h. The surface gust front is represented by the dashed contour.

4. INTERPRETATION

We attribute these differences in structure to the existence of the MAUL, and to the different manner in which the MAUL is perturbed. The environmental air flowing into the squall line is initially laminar in both simulations; when the environmental air ascends over the cold pool, it saturates and becomes statically unstable. Turbulent eddies then develop and overturn the unstable layer, but the character of the turbulence in the two simulations is obviously very different.

In simulation NO-PERT, it takes ~20-30 min for deep convective cells to develop, when considering a Lagrangian trajectory from the cold pool nose to the deep cells. In this case, the cells of ~3 km in scale are the fastest growing mode. The source for this 3 km spacing is clearly not the initial environment, because it has no perturbations. The lack of any preferred scale of forcing in the environment is confirmed by calculations of spectra in the environment ahead of the squall line.

This ~3 km spacing is unexpected. Theory indicates that the smallest horizontal scales should grow faster in a statically unstable layer. Hence the simulations suggest that another process is acting to perturb the MAUL at scales of ~3 km.

In simulation WITH-PERT, turbulent eddies emerge almost immediately after the MAUL is formed. Because the grid spacing (125 m) is much smaller than the unstable layer depth (1,500 m), this simulation contains resolved turbulent eddies at a spectrum of scales. These eddies are able to grow quickly because of the random thermal perturbations in the environment. This simulation confirms the theory that the smallest horizontal scales grow the fastest when all scales are given an equal chance to grow. That is, the environmental perturbations have a flat spectrum in wavenumber, i.e., perturbations of all spatial scales have equal amplitude. But the smallest scales emerge first, as theory suggests.

Table 1. Statistics from the two simulations.

	Without random perturbations	With random perturbations
0-3 h condensation ($\times 10^{10}$ kg)	5.3	5.2
0-3 h rainfall ($\times 10^{10}$ kg)	1.5	1.2
Precipitation efficiency	0.28	0.23

However, these small eddies do not immediately stabilize the MAUL; they have short lifetimes, and act only locally. When eddies on the scale of the MAUL depth finally become intense, they overturn the entire MAUL and stabilize the layer.

Although the small eddies are not directly responsible for stabilizing the MAUL, they do play a role in the final structure. That is, the small eddies enhance entrainment and dilute the cores of the large convective cells. This process explains the main differences in the overall system structure in the two simulations. In NO-PERT, big, strong, undilute cells develop first, and small eddies form later; whereas in WITH-PERT, the small eddies form first and dilute the big cells that form later. The existence of perturbations in the environment of WITH-PERT explains why the small eddies are able to develop quickly in this simulation.

5. CONCLUSIONS

This study has identified two factors that can affect the structure of convective cells in MCSs. The first factor is the formation of deep, wide moist absolutely unstable layers (MAULs). This condition is most likely met in upshear-tilted squall lines, where the environmental flow becomes quasi-horizontal over the cold pool. The second factor is the introduction of perturbations into the MAUL from the environmental inflow. Only two environmental states were studied herein: one without perturbations; and one with a white noise spectrum, in which perturbations of all scales have equal amplitude. The results confirm the theory that, when given an equal chance, the horizontally smallest perturbations will grow the fastest.

We surmise that the runs with random perturbations are more representative of the actual atmosphere, which is

constantly perturbed by variations in terrain, land use, and boundary-layer eddies. It is unclear whether a white noise spectrum is possible in the atmosphere; however, the existence of a wide spectrum of perturbations seems likely.

On the other hand, there is some evidence that plumes exist in some observed MCSs, although they have spacings larger than ~3 km. The present simulations suggest that preexisting perturbations are likely to be a determining factor in the existence and spacing of plume-like overturning in squall lines with MAULs. There might be instances when perturbations of a certain scale essentially dictate the spacing of cells in the convective region. For example, boundary layer rolls (i.e., cloud streets) might be a mechanism to perturb the convective region at a scale > 3 km (e.g., Atkins et al., 1995; Fovell and Dailey, 2001; Peckham et al. 2004).

Acknowledgments

All figures were created with the Grid Analysis and Display System (GrADS). Support was provided by NCAR's Advanced Study Program. NCAR is supported by the National Science Foundation.

REFERENCES

Atkins, N. T., R. M. Wakimoto, and T. M. Weckwerth, 1995: Observations of the sea-breeze front during CaPE. Part II: Dual-Doppler and aircraft analysis. *Mon. Wea. Rev.,* **123,** 944-969.

Bryan, G. H., and J. M. Fritsch, 2002: A benchmark simulation for moist nonhydrostatic numerical models. *Mon. Wea. Rev.,* **130**, 2917-2928.

Deardorff, J. W., 1980: Stratocumulus-capped mixed layers derived from a three-dimensional model. Bound.-Layer Meteor., 18, 495-527.

Fovell, R. G., and P. S. Dailey, 2001: Numerical simulation of the interaction between the sea-breeze front and horizontal convective rolls. Part II: Alongshore ambient flow. *Mon. Wea. Rev.,* **129,** 2057-2072.

Kessler, E., 1969: On the Distribution and Continuity of Water Substance in Atmospheric Circulation, Meteor. Monogr., No. 32, Amer. Meteor. Soc., 84 pp.

Peckham, S. E., R. B. Wilhelmson, L. J. Wicker, and C. L. Ziegler, 2004: Numerical simulation of the interaction between the dryline and horizontal convective rolls. *Mon. Wea. Rev.,* **132,** 1792-1812.

Weisman, M. L., and J. B. Klemp, 1982: The dependence of numerically simulated convective storms on vertical wind shear and buoyancy. *Mon. Wea. Rev.,* **110,** 504-520.

Wicker, L. J., and W. C. Skamarock, 2002: Time splitting methods for elastic models using forward time schemes. *Mon. Wea. Rev*., **130**, 2088-2097.